Acta Cryst. (1976). A**32**, 334

The Structure of Star Opals

BY J. V. SANDERS

CSIRO Division of Tribophysics, University of Melbourne, Parkville, Victoria, 3052, Australia

(*Received* 16 *June* 1975; *accepted* 24 *October* 1975)

Optical diffraction patterns have been obtained from a set of unusual gem opals from Idaho, U.S.A. The formation of star patterns in them is described, and the structure producing the stars is deduced from optical diffraction. The arrangement of particles is different from that found previously for Australian opals.

Introduction

The play of colours in gem opal has been shown to be caused by diffraction of white light by voids, naturally occurring between close-packed spheres of silica and arranged in a three-dimensional scattering array within the opal. The diffraction splits white light into the colours of the spectrum. The range of wavelengths which can be seen in an opal generally depends upon the size of the spheres, and all colours of the visible spectrum appear only if the diameters of the spheres are greater than about 250 nm (Sanders, 1964). An analysis of optical diffraction patterns showed that in most Australian opals the particles were in a close-packed arrangement which was randomly faulted on one set of close-packed planes so as to be neither cubic nor hexagonal in general. This faulting produces a set of parallel reciprocal lattice rods and lines of spots in reciprocal space (Sanders, 1968). Streaks of colour are formed by the rods cutting Ewald spheres corresponding to the various colours in the spectrum.

A recent report (Waller, 1974) describes some 'star opals', said to be unique to a source in Idaho, U.S.A. Their optical diffraction patterns have been found to contain strong intersecting 'rays' of colour confirming that the gems are justifiably called 'star opals'. These diffraction patterns are described below, and the packing arrangements which produce them are deduced; they are different from those found previously for Australian opals.

Experimental

Opal specimens

Diffraction patterns were obtained from 19 triplets exhibiting stars, selected from samples kindly provided by Mr Martin L. Meigs, President of the Idaho Opal and Gem Corporation, Pocatello, Idaho. A triplet is manufactured by cementing a thin wafer of opal onto a black backing, and covering it with a cap of quartz. This arrangement is sketched in Fig. 1. A number of uncapped samples were examined by optical and electron microscopy.

Apparatus

The optical apparatus, Fig. 2, has been described previously (Sanders, 1968). The opals were cemented onto holders which could be attached to a goniometer, with which the opal could be rotated about two orthogonal axes passing through its centre. The goniometer was mounted with the opal at the centre of a translucent flask, containing a small transparent window to admit light from a quartz–iodine lamp, focused on the back surface of the flask (Fig. 2). The flask was filled with dekalin to minimize distortion by refraction; however, there are small differences in the refractive indices (μ) of opal, quartz and dekalin (nominally $\mu =$ 1·45, 1·54, 1·47 respectively) which could produce systematic errors in measurements of angles of diffraction within the diffracting component, the opal. Consequently in these experiments more emphasis was placed on the wavelengths of the colours, assessed by comparison with a standard spectrum, than on angles measured on the goniometer. The wavelengths of some

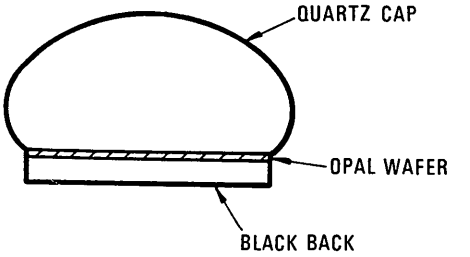

Fig. 1. Diagram showing construction of an opal triplet.

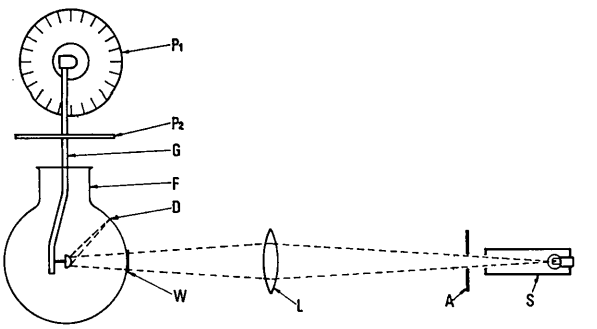

Fig. 2. Sketch of diffraction apparatus; P_1P_2, protractors; G, goniometer; F, flask; D, diffraction spot on surface of flask; W, window for admitting incident light; L, lens; A, aperture; S, light source.

colours such as blue and yellow can be estimated this way to within about ±1%, but the broad band of green, for example, makes an estimate of wavelength in the range 510–540 nm less accurate.

The specimens were adjusted to symmetry positions and the wavelengths of the colours of the diffraction features estimated. Angles of rotation to other symmetry positions were also measured. In this way that part of reciprocal space covered by the visible spectrum could be examined quantitatively.

The appearance of the gems themselves and some typical diffraction patterns were recorded on colour film.

Results

Specimens not giving 'single-crystal' patterns in the optical diffractometer were rejected. There were superficially three different types of diffraction pattern, and the specimens were grouped accordingly. The first group gave single streaks of colour at 60° intervals as the opal was rotated, as found previously for most Australian opals (Type I, Sanders, 1968). This gives these gems an appearance of chatoyancy, but does not produce a star. Consequently, they will not be considered here.

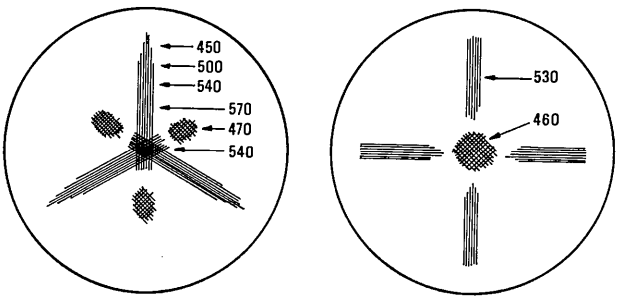

(*a*) (*b*)

Fig. 4. Sketches of the appearance of diffraction patterns from opals in Group *A*. The pattern in (*a*) is given at normal incidence and produces the characterisitc three-ray star; (*b*) appears when the opal is rotated by about 55°. The numbers give the wavelengths of the colours (in nm) for a typical specimen.

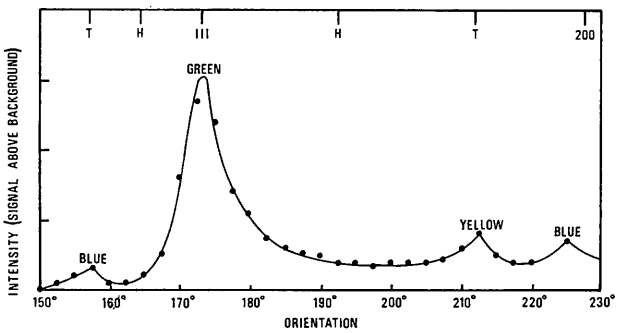

Fig. 5. Intensity distribution along a streak forming one of the rays of a star, measured at a fixed point near the entrance window, with a spot photometer, as a function of orientation, for an opal giving a three-ray star. The letters along the top show positions of maxima expected from single crystal f.c.c. 111, 200 reflexions, hexagonal, *H*, and twin orientations, *T*.

Group A: *three-ray star* (*nine specimens*)

At normal incidence these gave a pattern of three strong streaks, symmetrically placed and intersecting at a strong spot. The colour in the streak increased in wavelength away from the spot and then decreased again. The streaks extended weakly through the point of intersection to give a tail of shorter wavelengths. A photograph of a typical pattern is reproduced in Fig. 3(*a*). The significant features of the pattern are sketched in Fig. 4(*a*), where the colours for a typical example are indicated by their wavelengths. The three streaks were frequently not equally intense.

The intensity variation along the streak was measured by focusing a spot photometer on a spot as near as possible to the entrance window of the flask, and orienting the opal so that when it was rotated about a vertical axis, the streak traversed across that spot. The output of the photometer is shown plotted as signal above background as a function of orientation for a typical specimen in Fig. 5. The positions of intensity maxima expected from cubic 111 and 200 reflexions, hexagonal close-packed (*H*), and cubic twin orientations (*T*), are marked along the top. This plot shows that there is a strong asymmetry in the intensity distribution in the streak on the two sides of the central maximum. The intensity of the peak at the twin positions varied between samples. The colours observed at the positions of the maxima are shown for a typical specimen.

Rotation of the opal in one direction about an axis perpendicular to a streak, so that the direction of incidence followed along the intense part of the streak produced a spot with fourfold symmetric rays, pointing towards but stopping about 20° away from the spot. Its appearance is sketched in Fig. 4(*b*). Rotation in the opposite direction produced another spot with symmetric threefold streaks, similar to that at normal incidence.

A convenient way to describe this diffraction pattern is to plot stereographically the position of the opal when it produces a back diffraction colour ($2\theta=\pi$). Fig. 6 shows a sketch of such a plot for one of these opals, with numbers giving the wavelengths of the colours for a typical example.

The colours of the spots at the centres of the three- and fourfold rays had wavelengths in the ratio 1·15:1 (*e.g.* green, $\lambda=550$ nm and indigo, $\lambda=480$ nm). This is equal to the ratio of the spacings of (111) and (200) planes in a cubic system ($2/\sqrt{3}$). The angle through which the opal was turned to produce back diffraction from the spots was 61–65° between spots of threefold symmetry, and 50–54° between three and fourfold symmetry spots.

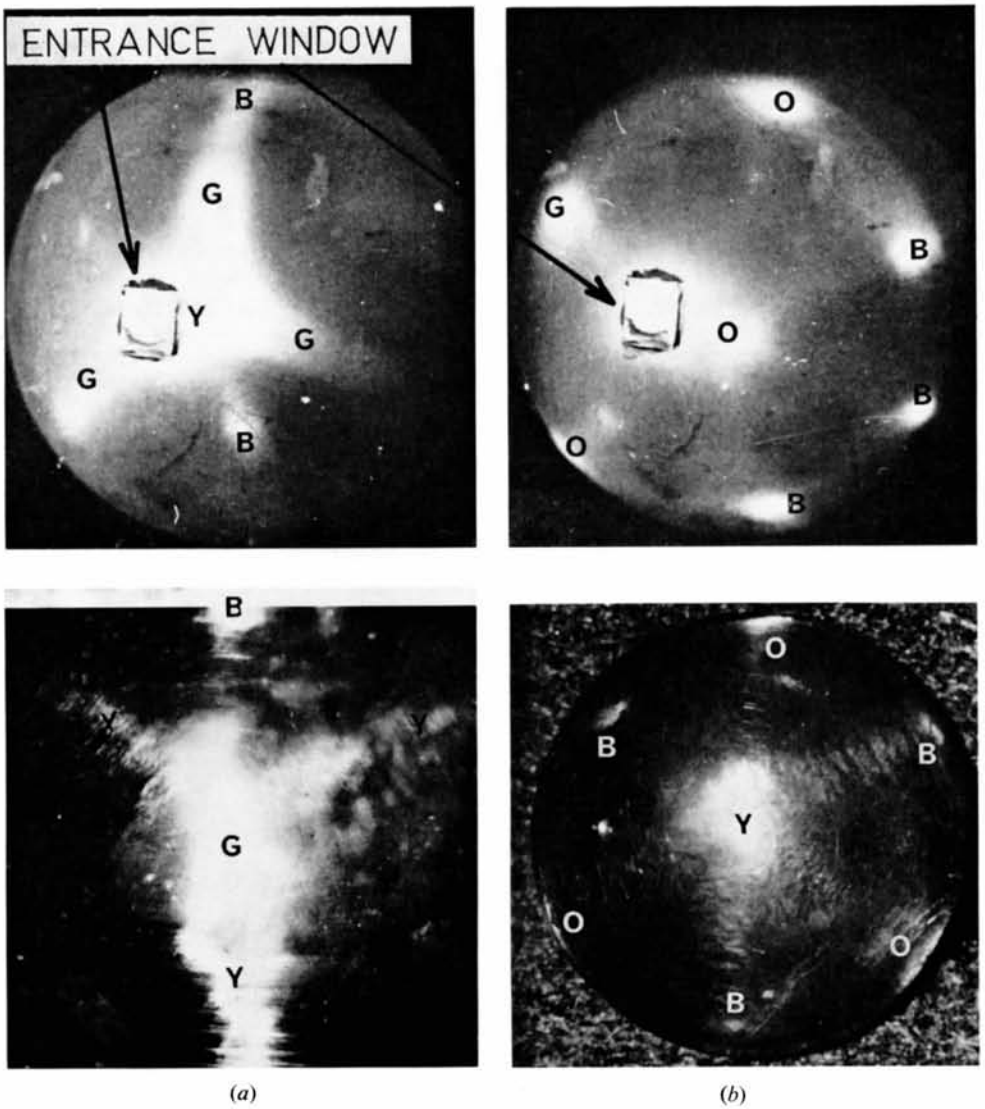

(*a*) (*b*)

Fig. 3. Photographs of diffraction patterns and macrophotographs of Idaho star opals. The opal has been rotated slightly away from the symmetry position in order to show the central reflexion in the diffraction patterns. Colours are indicated by letters: *O* orange, *Y* yellow, *G* green, *B* blue. (*a*) Three-ray star. (*b*) six-point star.

[*To face p.* 335

Group B: *six-point patterns* (*ten specimens*)

The optical diffraction patterns were dominated by strong spots, with trigonal symmetry in the symmetrical orientation. There was a central spot, surrounded by two sets of three or six spots symmetrically displaced about the centre. The wavelengths of the colours of the spots are listed in Table 1. There were three or six weak rays radiating from the centre towards the spots. The appearance of two types of pattern with this arrangement is sketched in Fig. 7. All colours changed systematically as the opal was rotated. The overall appearance of a typical specimen under vertical illumination is shown in the macrophotograph in Fig. 3. Under these conditions, the outer set of three orange spots is only just visible.

Electron microscopy

The specimens used for diffractometry were finished gems, and hence could not be examined by electron microscopy. However, an unpolished chip, with a plane highly-coloured face was obtained and examined in the optical diffractometer. It gave a three-ray star, with the wavelength of the central reflexion at the symmetrical position estimated as 590 nm, and the corresponding wavelength for the spot with fourfold symmetry was 500 nm.

A replica of an etched chip of this specimen was examined in an electron microscope, and fields containing close-packed rows of particles recorded. These gave a particle diameter, averaged over about ten particles in a row, of $2r=235$ nm, using the nominal value for the magnification of the instrument.

The rough opal from which suitable pieces are selected for the production of Idaho star opals consists of horizontal bands of opal up to 1mm thick, distinguishable by eye because they have different patterns of colour. An examination by electron microscopy of a section through one of the banded specimens showed that the spheres were the same size within the bands, but varied from 100 to 700 nm in diameter in the various bands.

Optical microscopy

At a magnification of about 100× on a stereomicroscope, a gem exhibiting a three-ray star can be viewed in the diffracted light from the rays of the star, and by tilting the stone around to optimum positions, at about 20° from normal incidence, each ray produces an image containing fine, parallel straight lines or bands running normal to the direction of the ray. Many of the lines terminate in the field of view, and their density is not the same for each ray. This appearance is just apparent in the macrophotograph (×5) of the three-ray star in Fig. 3. This also shows that one streak is much more intense than the other two.

Interpretation

Group A

The diffraction patterns consisted of spots and intense streaks. The wavelengths of the colours and the angular relationships between spots, Fig. 6, (the 10° discrepancy is probably due to refraction at the quartz/dekalin interface) are consistent with a body-centred cubic reciprocal lattice (corresponding to a face-centred lattice in real space) with rods in three of the ⟨111⟩ directions through the 111 reciprocal lattice points. Figs. 5 and 6 have been indexed accordingly.

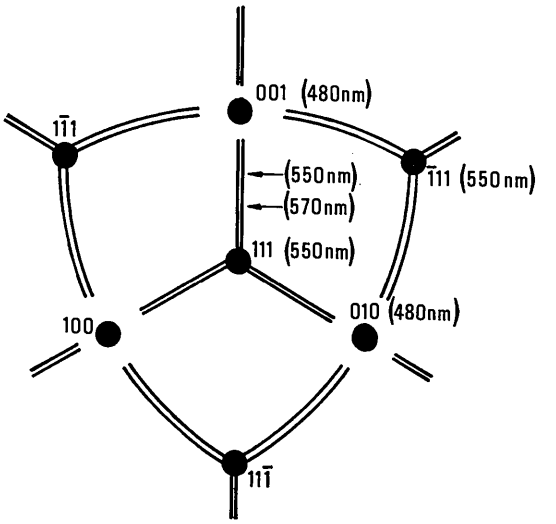

Fig. 6. Stereographic plot of the positions of a star opal from Group *A*, for which diffraction occurs. The lines correspond to the rays in the stars; the numbers give the wavelengths of colours (in nm) for a typical specimen.

Table 1. *Wavelengths, in* nm, *of the colours of diffraction spots from opals in Group B in the symmetry orientation*

The calculated values depend upon the index given to the central reflexion (Pole).

	Observed			Calculated		
	Pole	Set 1	Set 2			
D	520, (333)	490	570	491, (422)	575, (133)	
H	540, (333)	500	580	510, (422)	595, (133)	
I	560, (333)	520	600	528, (422)	616, (133)	
J	490, (333)	470, 650	530	462, (422)	666, (311)	542, (133)
K	590, (333)	570	630	555, (422)	652, (133)	
L	490, (333)	470	480–600	462, (422)	666, (311)	542, (133)
M	480, (333)	480	530	452, (422)	530, (133)	
N	580, (222)	520	580	526, (422)	528, (311)	580, (022)
P	650, (222)	480, 650	590	479, (133)	592, (311)	650, (022)

The section through reciprocal space sketched in Fig. 8 shows how a streak is produced by a reciprocal lattice rod intersecting Ewald spheres for various colours of the visible spectrum. Experimentally the strong streak corresponds to that point where the rod is tangential (or nearly so) to the Ewald spheres – section *AB*. The section *BC*, cutting the spheres for shorter wavelengths at larger angles produces a weak tail to the streak, which is less easily observed.

The effect of stacking faults on X-ray diffraction patterns from f.c.c. crystals has been considered by Paterson (1952), Guinier (1963) and Kakinoki (1967). Their analyses, which should also apply to the case of optical diffraction, predict an asymmetric broadening about some of the reflexions; this is what produces the streaks observed here. The accompanying displacement of the maxima has not been detected in these simple measurements. The graph in Fig. 5 can only be taken as a qualitative measure of the intensity distribution, because of uncertainties in the spectral distribution of the source and in the response of the detector. However, it does show that there are maxima at positions corresponding to twinning on the {111} planes other than (111), but not at the hexagonal close-packed reciprocal lattice positions. The general behaviour of the intensity is consistent with that given by Paterson (1952) in his Fig. 5(*b*) for $0<\alpha<2/3-3$ (α is the fault probability).

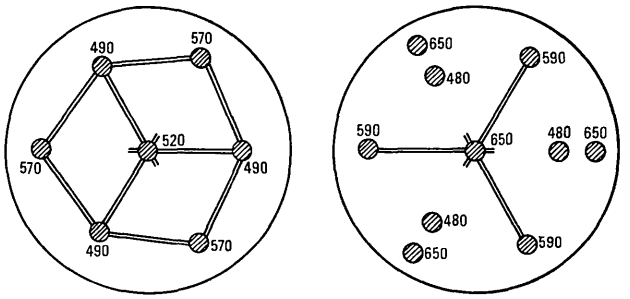

Fig. 7. Sketch of the appearance of two typical spot patterns from Group *B* opals (specimens *D* and *P*, Table 1). The numbers give the wavelengths of the colours of the spots (nm) and the lines represent streaks.

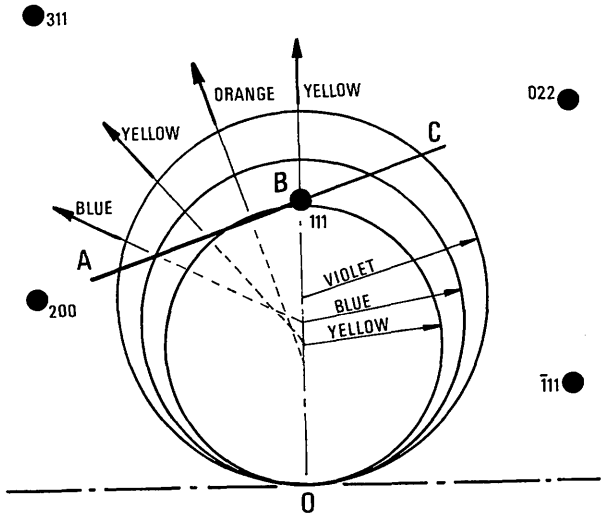

Fig. 8. Section through reciprocal space showing Ewald spheres for yellow, blue and violet colours, and the colour distribution along one ray of a star, produced by the intersection of the rod with the appropriate Ewald spheres. The streak from *A* to *B* is much more intense than from *B* to *C*. Situation at normal incidence for three-ray stars.

The diffraction spots from the three-ray star which was also examined by electron microscopy can therefore be indexed as 111 giving orange, $\lambda=590$ nm, and 200 giving green, $\lambda=500$ nm. Taking the refractive index as $\mu=1{\cdot}45$, these values give a lattice parameter, $a=352$ and 345 nm respectively. Taking the average as $a=348$ nm gives a particle diameter $2r=a/\sqrt{2}=247$ nm. The electron micrographs gave a value of $2r=235$ nm. The difference between these values is probably due to an error in magnification of the microscope. In fact, this seems to be a good method for calibrating the magnification of an electron microscope independently of a standard specimen.

Group B

By analogy with the X-ray case, the reciprocal lattice from layer structures consisting of close-packed spheres contains row lines (Farkas-Jahnke, 1973) parallel to the c^* axis (the reciprocal to the real-space c axis) through $hk0$ points, and whose separation is determined by the size of the spheres, because this determines the basal dimensions of the unit cell. The positions of the reciprocal lattice points on these row lines depends upon the stacking sequence of the layers. For Group *A* diffraction patterns, and for those observed previously for Australian opals (Sanders, 1968) at normal incidence only the central row line (through 000) was operating (Fig. 8), the other row lines being outside the Ewald spheres for visible light. By contrast, the Group *B* patterns at normal incidence contain sets of spots with trigonal symmetry about the central spot, showing that the first-order row lines [there are two sets, *plus* and *minus* respectively (Kakinoki, 1967) through $10\bar{1}0$ and $\bar{1}010$] must be operating also. The situation in reciprocal space [corresponding to the pattern in Fig. 7(*b*)] is sketched in Fig. 9. Points on the row lines corresponding to cubic and simple hexagonal stacking are indexed. In order that a visible colour appear from points on these row lines, their distance from the origin must be at least equal to the radius of the Ewald sphere for violet light ($\lambda=400$ nm), *i.e.* $r/3>400\times 1{\cdot}45$, or $r>335$ nm (r is the sphere radius, and 1·45 is the refractive index of opal). The appearance of colours of longer wavelength, as observed, (Table 1) implies that the spheres are even larger. This is about three times the size of the particles in the opals in Group *A*, and in the Australian opals studied previously (Sanders, 1968).

The patterns have trigonal symmetry so that the stacking sequence is not hexagonal, but may be cubic or some longer-range order. Table 1 lists the calculated wavelengths which would be observed for cubic stacking. The agreement with observed values is sufficiently good to identify the positions on the row-lines of the reciprocal lattice points which are operating. It suggests that the stacking sequence is cubic, although there may be another sequence which would also give these points a non-zero structure factor.

In these patterns the streaks are weaker than those in Group *A* (Fig. 2), and the most prominent go from the central beam towards the 422 or 311 reciprocal lattice points. These are cubic ⟨111⟩ directions, and the effect is therefore consistent with a cubic packing with faulting on the three of the {111} planes inclined to the surface of the opal. The extent of the faulting must frequently be different on the three sets of planes, because the intensities of the streaks are usually different. A rod normal to the surface would produce a streak through the 022 reflexion. This is not observed. This fact, together with the consistent observation of threefold rather than sixfold symmetry, shows that there is an absence of faulting and twinning on the close-packed planes parallel to the exposed face.

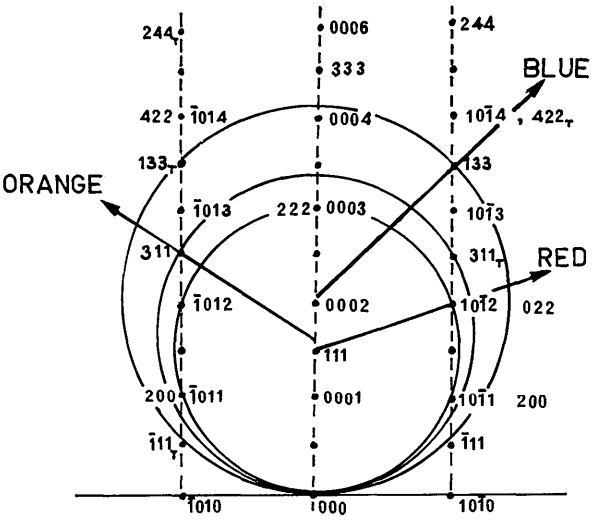

Fig. 9. Section through reciprocal space for six-ray stars, showing how the spots come from reciprocal lattice points on row lines parallel to c^*, through $10\bar{1}0$ and $\bar{1}010$. It shows that the diffracted beams corresponding to the diffraction pattern sketched in Fig. 7(*b*), come from untwinned, f.c.c. stacked layers.

Discussion

A theory for the formation of precious opal (Darragh, Gaskin, Terrell & Sanders, 1966) contains a step in the process in which uniformly sized silica particles settled into a crystal-like, close-packed array. A feature which distinguishes the Idaho opal is that in the unpolished material there are sequences of horizontal bands up to 1 mm thick containing uniformly sized spheres, and separated by one or more layers of silica. It seems likely that when this silica interface provided a smooth enough, horizontal surface onto which the particles in the layer above settled, they formed an extensively ordered hexagonal array. It has been observed that silica and latex particles settling onto the smooth glass surfaces of containers form such extensively ordered arrays (Alfrey, Bradford, Vanderhoff & Oster, 1954; Krieger & O'Neill, 1968). In the case of these Idaho star opals, when this happened the subsequent layers settled into a well ordered f.c.c. sequence. This seems to indicate that particles in next nearest layers interacted with each other. The minimum distance between next-to-nearest layers is $2r\sqrt{2}/\sqrt{3}=3{\cdot}27r$; thus this interaction must have extended over distances of at least 1μm for some of the samples examined here.

References

ALFREY, T., BRADFORD, E. B., VANDERHOFF, J. W. & OSTER, G. (1954). *J. Opt. Sci. Amer.* **44**, 603–609.
DARRAGH, P. J., GASKIN, A. J., TERRELL, B. C. & SANDERS, J. V. (1966). *Nature, Lond.* **209**, 13–16.
FARKAS-JAHNKE, M. (1973). *Acta Cryst.* B**29**, 407–413.
GUINIER, A. (1963). *X-ray Diffraction*, p. 234. San Francisco: Freeman.
KAKINOKI, J. (1967). *Acta Cryst.* **23**, 875–885.
KRIEGER, I. M. & O'NEILL, F. M. (1968). *J. Amer. Chem. Soc.* **90**, 3114–3120.
PATERSON, M. S. (1952). *J. Appl. Phys.* **23**, 805–811.
SANDERS, J. V. (1964). *Nature, Lond.* **204**, 1151–1153.
SANDERS, J. V. (1968). *Acta Cryst.* A**24**, 427–434.
WALLER, J. E. (1974). *Rock Gem.* Sept. 37.